Available online at www.sciencedirect.com
ScienceDirect
Journal of Structural Biology 160 (2007) 28–34
Journal of Structural Biology
www.elsevier.com/locate/yjsbi

# Crystal structure of mastoparan from *Polistes jadwagae* at 1.2 Å resolution

ShengQuan Liu [a,1], Feng Wang [a,1], Lin Tang [a], WenJun Gui [a], Peng Cao [a], XiaoQin Liu [a], Alice Wing-Sem Poon [b], Pang-Chui Shaw [b,*], Tao Jiang [a,*]

[a] *National Laboratory of Biomacromolecules, Institute of Biophysics, Chinese Academy of Sciences, 15 Datun Road, Chaoyang District, Beijing 100101, China*

[b] *Department of Biochemistry and Centre for Protein Science and Crystallography, The Chinese University of Hong Kong, Shatin, NT, Hong Kong, China*

Received 15 March 2007; received in revised form 28 May 2007; accepted 15 June 2007
Available online 23 June 2007

**Abstract**

Mastoparans, a group of amphiphilic tetradecapeptides, are the major peptides in social wasp venoms and possess a variety of biological activities. Here we report the first crystal structure of mastoparan from *Polistes jadwagae* (MP-PJ) at 1.2 Å resolution. The crystals belong to the space group $P2_1$ with eight molecules in an asymmetric unit. In contrast to the previous observations that the α-helical conformation only exists in the membrane-bound state of mastoparans, all of the MP-PJ molecules are in possession of the α-helical conformation even in the absence of trifluorethanol or detergents in the crystallization system. The high-resolution structure enables us to compare the conformation differences of MP-PJ with NMR results of other mastoparans. Together with biochemical results, we propose that the interactions between mastoparan molecules play an important role in forming the α-helical conformation, which is highly related to their biological activities.


*Keywords:* Mastoparan; Crystal structure; C-terminal amidated; Helical conformation

## 1. Introduction

Mastoparans are a family of amphiphilic tetradecapeptides and known to be the major peptides in many species of wasp venoms (Nakajima et al., 1986). They were originally discovered as the agents that induce histamine release from mast cells and later found to affect a variety of biological activities, including induction of secretion in different types of cells (Mizuno et al., 1998; Murayama et al., 1996; Ohara-Imaizumi et al., 2001; Straub et al., 1998; Wu et al., 1999; Yajima et al., 1997), hemolytic activity (Mendes et al., 2005), antimicrobial activity (Park et al., 1995), etc.

The biological activities of mastoparans have been ascribed to their ability to interact with the cell membrane surface, G proteins and calmodulin via the positively charged side of their amphipathic α-helical structure and these activities are associated with some types of post-transcriptional processing of their precursors, such as C-terminal amidation. This also occurs with other peptides, such as melittin, clavanin or penaeidins, etc. There are studies showing an increase in activity following amidation or, alternatively, an activity decrease when the amide is removed (Ali et al., 2001; Katayama et al., 2002; Sandvik and Dockray, 1999).

Structural studies on mastoparans with detergents, in a membrane-bound state, were mainly carried out by nuclear magnetic resonance (NMR) spectroscopy (Hori et al., 2001; Kusunoki et al., 1998; Ohki et al., 1991; Sukumar

* Corresponding authors. Fax: +86 10 64888510 (T. Jiang), fax: +852 26035123 (P.-C. Shaw).
*E-mail addresses:* pcshaw@cuhk.edu.hk (P.-C. Shaw), x-ray@sun5.ibp.ac.cn (T. Jiang).
[1] These authors contributed equally to this work.

1047-8477/$ - see front matter © 2007 Elsevier Inc. All rights reserved.
doi:10.1016/j.jsb.2007.06.005

et al., 1997; Yu et al., 2001). Combined with CD results, it revealed that mastoparans exhibit a random coil conformation in aqueous solution, whereas in trifluorethanol (TFE)- or detergents-containing solution, they adopt the amphipathic α-helical conformation (Chuang et al., 1996), and therefore it is speculated that the conformation of mastoparans could be induced from coil to helix upon binding to a membrane. However, NMR structures did not provide information on the intermolecular interactions between mastoparans or with other biological molecules.

In order to provide further insights into the conformational characteristics and the implications for its biological functions, attempts at crystallization of mastoparan analogues in 50% trifluorethanol-containing aqueous solution were reported (Canduri et al., 2000; Delatorre et al., 2001). However, no crystal structure of mastoparans has been reported yet.

Mastoparan from *Polistes jadwagae* (MP-PJ, VDWKK IGQHILSVL-$NH_2$) is similar to other mastoparans in activities and its preliminary crystallographic study was carried out in our laboratory (Wang et al., 2006). Here we report the crystal structure of MP-PJ, the first crystal structure of mastoparans, at 1.2 Å resolution. Our results reveal the detailed structural features of mastoparan in a membrane-free state, which provide new insights into the intermolecular interactions of mastoparans.

## 2. Materials and methods

### 2.1. Data collection and processing of heavy atom derivatives

The MP-PJ used in the experiments was purchased from Sigma Corp. and used without further purification. Crystallization conditions, X-ray data collection and processing of native MP-PJ at 1.2 Å resolution were described previously (Wang et al., 2006).

Potential heavy atom derivatives were screened and $K_2[PtCl_4]$ was identified as a promising candidate. 10 mM $K_2[PtCl_4]$ was added to the hanging drops of native MP-PJ crystallization system. Native crystals were soaked for different times, from 2 to 48 h.

Diffraction data of a derivative crystal were collected at 100 K with the paratone-N (Hampton Research Corp.) as cryo-protection on a MAR Research imaging plate scanner, using CuKα monochromatic radiation produced by a Rigaku RU-200 rotating anode X-ray generator. With an oscillation range of 3.0°, 480 images were collected and the raw X-ray diffraction data were processed to 1.45 Å resolution using the program DENZO and scaled with the program SCALEPACK (Otwinowski and Minor, 1997). The crystal is isomorphous with that of native MP-PJ and detailed data collection statistics are given in Table 1.

### 2.2. Structure determination of a heavy atom derivative

PHENIX (Python-based Hierarchical Environment for Integrated Xtallography, version 1.1a) (Adams et al., 2002) was used to solve the structure of the Pt derivative and 11 Pt atoms were identified with occupancies varying from 0.3 to 0.02. The program Coot (Emsley and Cowtan, 2004) was then used for model building and eight peptide chains were finally found in an asymmetric unit. The structure of native MP-PJ was solved by molecular replacement with the program MOLREP (Vagin and Teplyakov, 1997) from the CCP4 program suite (Dodson et al., 1997), using the refined structure of Pt derivative in an asymmetric unit (eight peptides) as the search model. Five percents of the observed reflections were flagged for the calculation of $R_{free}$, which was also applied in the refinement of the Pt derivative structure. The CNS program (Brunger et al., 1998) was used to refine coordinates and B-factors, and finally to add sulfate ions and water molecules. All model building was performed manually with the program Coot (Emsley and Cowtan, 2004). The final model contains 112 residues in eight peptide chains, 3 sulfate ions and 144 water molecules and its quality was evaluated using PROCHECK (Morris et al., 1992). Details of the structure refinement are given in Table 2. CCDC 639374 contains the supplementary crystallographic data for this paper. These data can be obtained free of charge from The Cambridge Crystallographic Data Centre via www.ccdc.cam.ac.uk/data_request/cif.

Table 1
Data collection and processing statistics of MP-PJ Pt derivative

| | |
|---|---|
| Resolution range (Å) | 100.0–1.45 (1.50–1.45) |
| Space group | $P2_1$ |
| Cell dimensions (Å) | |
| *a* | 22.1 |
| *b* | 59.4 |
| *c* | 37.3 |
| *β* (°) | 101.1 |
| Vm ($Å^3$/Da) | 1.91 |
| Number of molecules in the unit cell | 8 |
| Solvent content (%) | 35.6 |
| Total number of reflections | 537,014 |
| Number of unique reflections | 14,706 |
| % completeness | 86.9 (63.8) |
| $R_{merge}$ | 0.062 (0.421) |
| Output $<I/\mathrm{sig}I>$ | 56.5 (8.64) |

Note: Values in brackets are for the last resolution shell.

### 2.3. Surface plasmon resonance study

Real-time binding by surface plasmon resonance was carried out on a BIAcore 3000 instrument. The SPR signal was expressed in relative response units (RU); that is, the response obtained in a control flow channel was subtracted. The eluent contained 150 mM NaCl, 50 mM Hepes (pH 7.4), 1 mM $CaCl_2$ and 0.005% Tween 20.

In the comparison of MP-PJ and MP-PJ-$COO^-$ to interact with calmodulin, biotinylated calmodulin was immobilized over the streptavidin surface of a SA chip which had been activated with three consecutive injections of 1 M NaCl containing 50 mM NaOH, until the signal reached

Table 2
Structure refinement statistics of native MP-PJ

| | |
|---|---|
| Space group | $P2_1$ |
| Cell dimensions (Å) | |
| *a* | 22.1 |
| *b* | 59.5 |
| *c* | 37.2 |
| *β* (°) | 101.4 |
| Resolution range (Å) | 30–1.2 (1.24–1.2) |
| Total number of reflections | 180,667 |
| No. of unique reflections | 26,984 |
| % completeness | 93.7 (89.0) |
| $R_{merge}$ | 0.047 (0.256) |
| Output <*I*/sig *I*> | 46.2 (5.7) |
| $R_{working}$[a] | 18.2 |
| $R_{free}$ (5% data) | 20.1 |
| R.m.s.d. bond distance (Å)[b] | 0.003 |
| R.m.s.d. bond angle (°)[b] | 0.909 |
| Number of peptide atoms | 928 |
| Number of solvent molecules | 144 |
| Number of sulphate molecules | 3 |
| Average B-factors of all no hydrogen atoms (Å) | 9.82 |
| Ramachandran plot (excluding glycines) | |
| Residues in most favored regions | 89 (92.7%) |
| Residues in additional allowed regions | 7 (7.3%) |

Note: Values in brackets of the upper block are for the last resolution shell and all refinement and calculation of *R* factor were performed in CNS using all reflections.

[a] $R_{working} = \sum_{hkl}|F(hkl)_{obs} - <F(hkl)_{calc}>|/\sum_{hkl}F(hkl)_{obs}$.

[b] R.m.s.d., root mean square deviation.

~800 RU. Binding was evaluated with peptides of 80 μM at a continuous flow of 30 μL/min at 25 °C.

### 2.4. Circular dichroism spectrum of MP-PJ and MP-PJ-COO$^-$

MP-PJ and MP-PJ-COO$^-$ were dissolved in crystallization solution that contained 0.036 M ammonium sulfate, 0.06 M sodium cacodylate and different concentrations of PEG1500, at pH 6.5, the concentrations of peptides varied from 0.3 to 0.8 mg/mL (we used up to 1.2 mg/mL protein). The CD spectra from 190 to 260 nm were determined by a Jasco J-810 spectrometer using a sample cell of 1 mm path length. Protein was scanned three times from 190 to 260 nm and CD signals were generated in a bandwidth of 1 nm at 1-s response time. Data pitch was set at 0.1 nM with the scanning at 100 nm per minute. The spectra were averaged and subtracted from buffer blank spectrum. Deconvolution of CD spectra of the various conformations was achieved using the CDNN program.

## 3. Results and discussion

### 3.1. Overall crystal structure

There are eight molecules in an asymmetric unit (Fig. 1a). Four of them, molecules 1–4, are arrayed head to tail to form an antiparallel single-molecular layer. The other four molecules, 5–8, are also arrayed head to tail to form another single-molecular layer. Except for the first two residues, residues 3–14 in all these peptides adopt a well-defined amphiphilic α-helical conformation and the axes of α-helixes in these two layers are roughly perpendicular to each other.

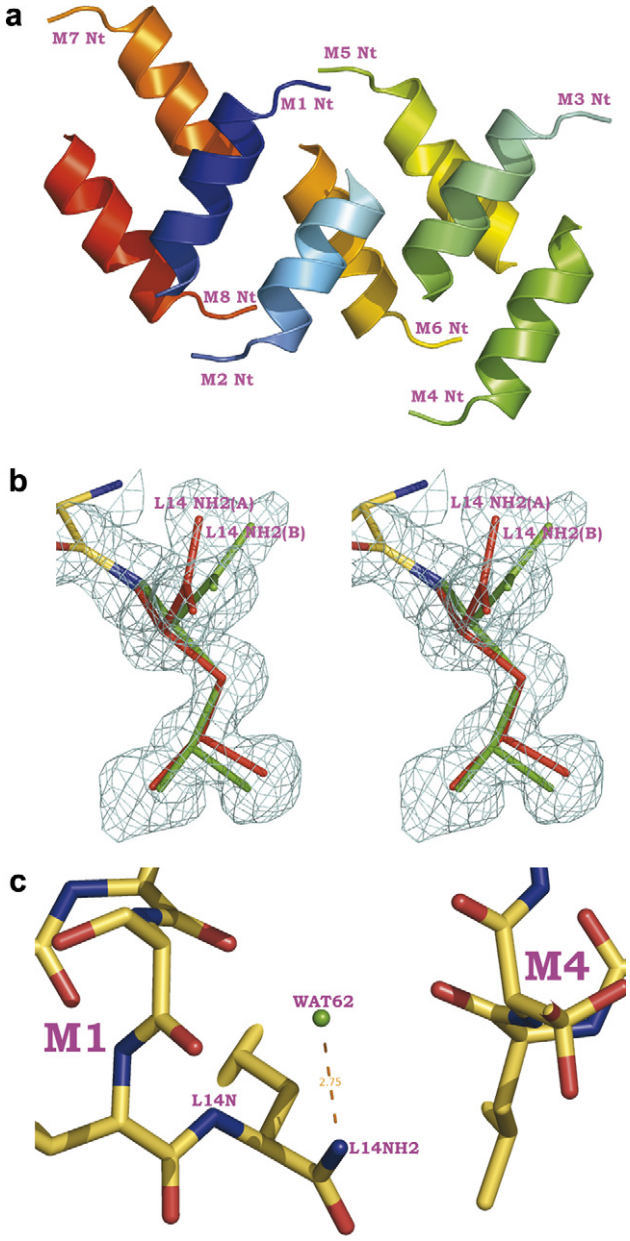


Fig. 1. Overall structure and C-terminal conformations of MP-PJ. Molecules 1–8 are labeled as M1 to M8, respectively, and the N-terminal of peptides are labeled as Nt. (a) Packing of the eight peptides in the asymmetric unit to form two single-molecular layers that are vertical to each other. The forward layer is composed of molecules 1–4 and the back layer is 5–8. (b) C-terminal dual conformations of molecule 2. Conformation A is expressed in red and conformation B is in green. The dual amide NH2 is at the top of the 2fo-fc electron density map at 1.0σ level. (c) C-terminal conformation of molecule 1. Leu14 NH2 forms only one hydrogen bond with a water molecule (the 62th water molecule labeled as Wat62) and Leu14 N does not form any hydrogen bonds.

In our structure, the amphiphilic α-helical conformation is composed of hydrophilic side-chains (Asp2, Lys5, Gln8,

His9 and Ser12) on one lateral surface and hydrophobic side-chains (Val1, Trp3, Ile6, Ile10 and Leu14) on the other side. It is consistent with the model that upon reaching the membrane, the hydrophilic side interacts with the membrane surface firstly and then the hydrophobic side permeates the membrane via the "barrel stave" mechanism or the "carpet" mechanism (Shai, 2002). This explains why the completeness of the amphiphilic α-helical conformation is of extremely importance for its interaction with membrane.

The α-helical structures of molecules 3–8 are similar; the main chain RMS deviations between each other are ranged from 0.19 to 0.79 Å, based on residues 3–14. In these structures, the C-terminal amides (Leu14 NH2) form hydrogen bonds with the main chain carbonyl oxygens of Leu11 (Leu11 O) in the same molecule. The O–N distances are in the range from 2.84 to 3.15 Å. Hydrogen bonds are also formed between the main chain nitrogens of the C-terminal Leu14 (Leu14 N) and the main chain carbonyl oxygens of the intra-molecular Ile10 (Ile10 O). The latter O–N distances range from 2.81 to 2.93 Å. These two hydrogen bonds help to keep the C-terminal residues in the α-helix. The structures of the six molecules are similar to those revealed by an NMR study on eumenine mastoparan-AF (Sforca et al., 2004).

### 3.2. Structures of molecules 1 and 2 have a new C-terminal conformation

The C-terminal Leu14 of molecule 2 has dual conformations (Fig. 1b). Conformation B is similar to those in molecules 3–8, and the two hydrogen bonds, Leu14 NH2 ∼ Leu11 O, 2.69 Å and Leu14 N ∼ Ile10 O, 2.98 Å are all present.

For conformation A, though the hydrogen bond between Leu14 N and Ile10 O (2.95 Å) is retained, the distance between Leu14 NH2 and Leu11 O is 3.59 Å, which is beyond the hydrogen bond range. However, two new hydrogen bonds are formed between Leu14 NH2 and the main chain carbonyl oxygens nearby, Ser12 O and Val13 O, with distances of 3.19 and 3.04 Å, respectively. The C terminus is still in the helical conformation.

It is more interesting and surprising that molecule 1 has a different C-terminal conformation, with all hydrogen bonds mentioned above being absent (Fig. 1c). In this molecule, Leu14 NH2 only forms a hydrogen bond with a water molecule and Leu14 N does not form any hydrogen bonds. The nearest distance between Leu14 N and the carbonyl oxygens all around is above 3.50 Å. However, residues 3–14 still form a helical conformation, though Leu14 has a slightly deviation from the helical conformation compared to that in molecules 3–8. Therefore, it is likely that conformation A of molecule 2 is a transition state between the conformation of molecule 1 and molecules 3–8.

### 3.3. Conformation and charge interaction

In the NMR structure of the C-terminal unamidated mastoparan, the C-terminal residue does not form any hydrogen bonds with other residues and the whole molecule is divided into a two helical stretch conformation (Sforca et al., 2004). In our X-ray crystal structure, although the amidated C-terminal of molecule 1 does not have any hydrogen bonds with residues 1–13, the whole molecule is in one continuous helical conformation. It is likely that the existence of an amidated C-terminal residue has an important impact on the helical conformation.

It was reported that mastoparan can bind to calmodulin with high affinity (Malencik and Anderson, 1983). Therefore, we used surface plasmon resonance to measure the interaction of calmodulin with MP-PJ and MP-PJ-$COO^-$. The results revealed that the interaction between calmodulin and MP-PJ-$COO^-$ is far weaker than that between calmodulin and MP-PJ (Fig. 2), suggesting that C-terminal amidation of mastoparan is crucial for associating with its target protein, and that this may in turn influence its biological activities.

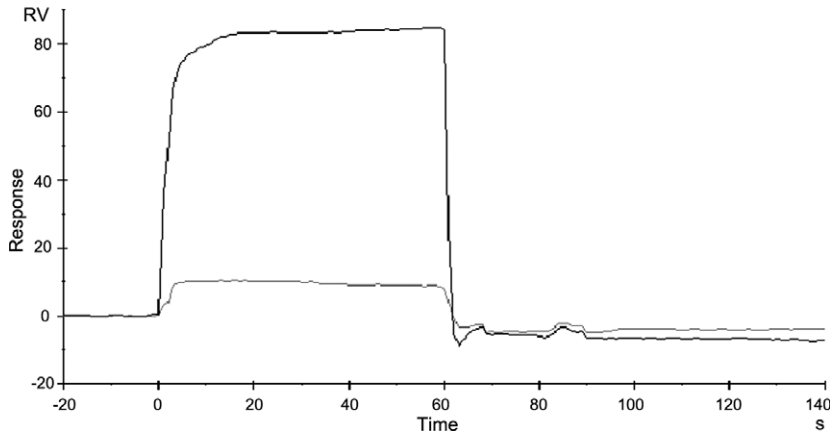


Fig. 2. Surface plasmon resonance study on the interaction between MP-PJ/MP-PJ-$COO^-$ and CaM. The darker line is for MP-PJ and the lighter one for MP-PJ-$COO^-$.

### 3.4. Circular dichroism spectrum and intermolecular interactions

To better understand the conformation of mastoparan, the secondary structures of MP-PJ and MP-PJ-COO$^-$ were detected by a CD spectrometer. Interestingly, there was almost no difference in the CD spectra of MP-PJ and MP-PJ-COO$^-$ in the indicated conditions. At a peptide concentration of 0.5 and 0.8 mg/mL, the contents of α-helical conformation of both peptides are around 35% and 38%, respectively. Addition of PEG1500 up to 12% (half of the concentration as in the crystallization reservoir solution) had little influence on the α-helical contents.

Given the higher helical content and higher concentration of mastoparan in the crystal, we propose that the intermolecular interactions observed in the crystal structure contribute to the formation and maintenance of α-helical conformation. For the intermolecular interaction, this is mainly composed of hydrogen bonds with the aid of solvent water. All of the seven polar residues have the ability to form hydrogen bonds directly with other residues and two of the seven nonpolar residues, Val1 and Leu11, also hydrogen bonded with other residues (shown in Table 3). The C-terminal amides of molecules 3–8 (bold in Table 3) form hydrogen bonds with nearby residues of other monomers, four of them (molecules 4–7) are hydrogen bonded to the main chain carbonyl oxygens of Leu11 or Gln8 (Fig. 3a) while the other two are bonded to the side-chain carbonyl oxygens of Gln8 residues (Fig. 3b). For the C-terminal amides of molecules 1 (Fig. 1c) and 2 with conformation A or B (Fig. 3c), they are only hydrogen bonded to water molecules but not to residues from other peptides. Since the C-terminals of molecules 1 and 2 are more flexible than those in molecules 3–8, we propose that the hydrogen bonds between the C-terminal amides and carbonyl oxygens of other cellular molecules may also play a role in the α-helical conformation of mastoparans.

Table 3
Hydrogen bonds between different molecules of mastoparan

| Molecules | Hydrogen bonds |
|---|---|
| M1 ~ M4 | **Leu11 O ~ Leu14 NH2**[a] |
| M1 ~ M6 | Lys5 NZ ~ Leu14 O |
| M1 ~ M7 | Val1 O ~ Lys4 NZ(A)[b], Lys5 O ~ Ser12 OG(A), Gln8 OE1 ~ Ser12 OG(B, C)[b], His9 ND1 ~ Ser12 O |
| M2 ~ M3 | **Gln8 OE1 ~ Leu14 NH2**, Gln8 NE2 ~ Ser12 O, Leu14 O(A, B) ~ Gln8 NE2 |
| M2 ~ M6 | His9 ND1 ~ Ser12 OG, Ser12 OG ~ His9 ND1 |
| M2 ~ M7 | Val1 N ~ Asp2 OD1 |
| M3 ~ M5 | Lys5 NZ ~ Gln8 OE1 |
| M3 ~ M6 | Ser12 OG(B) ~ His9 ND1 |
| M4 ~ M5 | Asp2 OD1 ~ Val1 N |
| M4 ~ M6 | Lys4 NZ ~ Val1 O |
| M4 ~ M7 | Gln8 OE1 ~ Lys4 NZ(B), Gln8 OE1 ~ Gln8 NE2 |
| M4 ~ M8 | Ser12 O ~ His9 ND1 |
| M5 ~ M8 | **Gln8 OE1 ~ Leu14 NH2**, Gln8 NE2 ~ Leu14 O, **Leu14 NH2 ~ Gln8 O** |
| M6 ~ M7 | **Leu11 O ~ Leu14 NH2**, **Leu14 NH2 ~ Leu11 O** |

[a] Hydrogen bonds formed by Leu14 NH2 are in bold type.
[b] (A, B, C), conformation A/B/C of the atom, same as in the Fig. 1b.

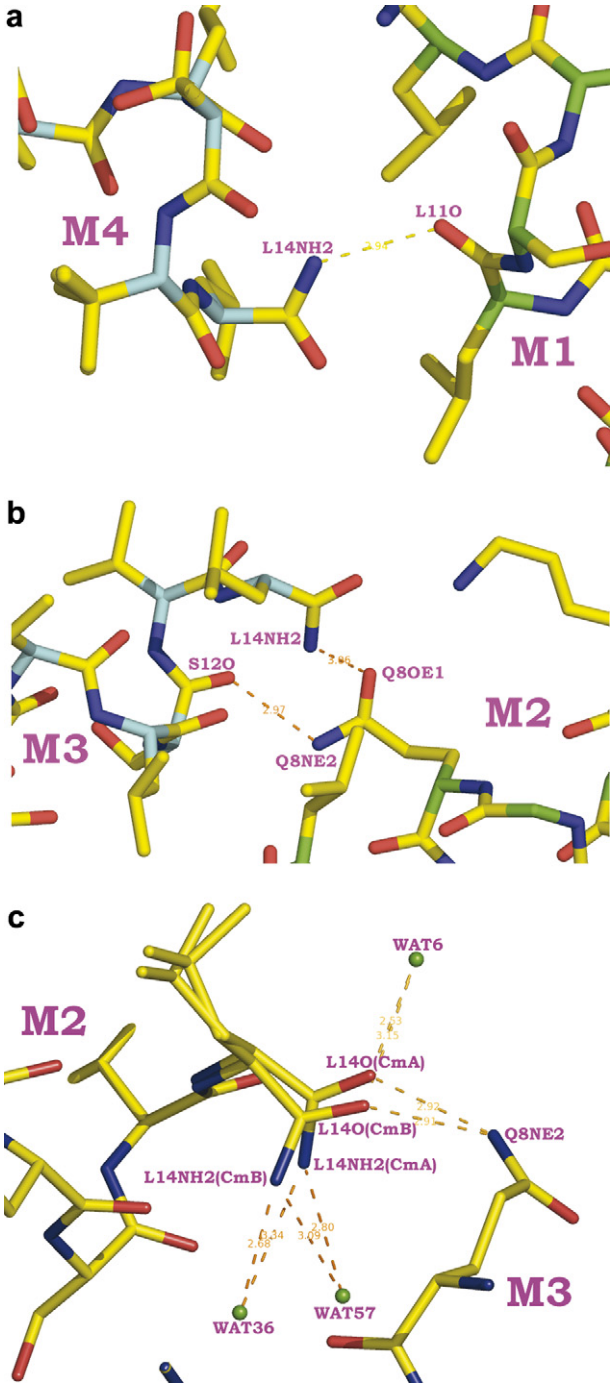


Fig. 3. Intermolecular hydrogen bonds of C-terminal amides. Molecules 1–4 are labeled as M1 to M4, respectively. (a) Intermolecular hydrogen bond of the C-terminal amide of molecule 4. It is similar for molecules 5–7. (b) Intermolecular hydrogen bond of the C-terminal amide of molecule 3. It is similar for molecule 8. (c) Intermolecular hydrogen bonds of the C-terminal amide of molecule 2, in both conformations. CmA and CmB represent conformations A and B, respectively. Water molecules are labeled according to the order of appearance in the structure.

## 4. Conclusion

Up to now, only solution structures of mastoparans have been determined by NMR spectroscopy and the α-helical conformation is found to exist in solutions contain-

ing trifluorethanol, SDS or other detergents, but not in aqueous solutions. Here we report the first crystal structure of mastoparan that adopts an α-helical conformation in the absence of TFE or detergents. Together with the CD results, we suggest that besides the mastoparan-membrane interaction, interaction between mastoparan and other molecules is also crucial for inducing the α-helical conformation. The observation that the interaction between calmodulin and MP-PJ is far stronger than that between calmodulin and MP-PJ-$COO^-$ suggested that the amidated C-terminal of mastoparan is crucial for associating with its target proteins, and thus influences its biological activities.

The present high-resolution structure of MP-PJ has also revealed the detailed extra- and intra-molecular interactions and identified determinants for maintaining the α-helical conformation. These structural informations can be helpful for designing mastoparan variants with different biological activities.

## Acknowledgments

We thank Yuan-Yuan Chen of the Institute of Biophysics for her assistance in BIAcore experiments. This project was supported by Grants from the National Key Basic Research Program (2006AA02A422 and 2004CB720000) and the National Natural Science Foundation of China (30300065). It was also supported by Synchrotron Radiation fund of Innovation Project of Ministry of Education. Work in Hong Kong was supported by a strategic grant from the Chinese University of Hong Kong.

## References

Adams, P.D., Grosse-Kunstleve, R.W., Hung, L.W., Ioerger, T.R., McCoy, A.J., Moriarty, N.W., Read, R.J., Sacchettini, J.C., Sauter, N.K., Terwilliger, T.C., 2002. PHENIX: building new software for automated crystallographic structure determination. Acta Crystallogr. D 58, 1948–1954.

Ali, M.F., Soto, A., Knoop, F.C., Conlon, J.M., 2001. Antimicrobial peptides isolated from skin secretions of the diploid frog, Xenopus tropicalis (Pipidae). Biochim. Biophys. Acta 1550, 81–89.

Brunger, A.T., Adams, P.D., Clore, G.M., DeLano, W.L., Gros, P., Grosse-Kunstleve, R.W., Jiang, J.S., Kuszewski, J., Nilges, M., Pannu, N.S., Read, R.J., Rice, L.M., Simonson, T., Warren, G.L., 1998. Crystallography & NMR system: a new software suite for macromolecular structure determination. Acta Crystallogr. D 54, 905–921.

Canduri, F., Delatorre, P., Fadel, V., Lorenzi, C.C.B., Pereira, J.H., Olivieri, J.R., Neto, J.R., Konno, K., Palma, M.S., Yamane, T., de Azevedo Jr., W.F., 2000. Crystallization and preliminary X-ray diffraction analysis of a eumenine mastoparan toxin: a new class of mast-cell degranulating peptide in the wasp venom. Acta Crystallogr. D 56, 1434–1436.

Chuang, C.C., Huang, W.C., Yu, H.M., Wang, K.T., Wu, S.H., 1996. Conformation of Vespa basalis mastoparan-B in trifluoroethanol-containing aqueous solution. Biochim. Biophys. Acta 1292, 1–8.

Delatorre, P., Olivieri, J.R., Neto, J.R., Lorenzi, C.C.B., Canduri, F., Fadel, V., Konno, K., Palma, M.S., Yamane, T., de Azevedo Jr., W.F., 2001. Preliminary cryocrystallography analysis of an eumenine mastoparan toxin isolated from the venom of the wasp anterhynchium flavomarginatum micado. Biochim. Biophys. Acta 1545, 372–376.

Dodson, E.J., Winn, M., Ralph, A., 1997. Collaborative computational project, number 4: providing programs for protein crystallography. Methods Enzymol. 277, 620–633.

Emsley, P., Cowtan, K., 2004. Coot: model-building tools for molecular graphics. Acta Crystallogr. D 60, 2126–2132.

Hori, Y., Demura, M., Iwadate, M., Ulrich, A.S., Niidome, T., Aoyagi, H., Asakura, T., 2001. Interaction of mastoparan with membranes studied by 1H-NMR spectroscopy in detergent micelles and by solid-state 2H-NMR and 15N-NMR spectroscopy in oriented lipid bilayers. Eur. J. Biochem. 268, 302–309.

Katayama, H., Ohira, T., Aida, K., Nagasawa, H., 2002. Significance of a carboxyl-terminal amide moiety in the folding and biological activity of crustacean hyperglycemic hormone. Peptides 23, 1537–1546.

Kusunoki, H., Wakamatsu, K., Sato, K., Miyazawa, T., Kohno, T., 1998. G protein-bound conformation of mastoparan-X: heteronuclear multidimensional transferred nuclear overhauser effect analysis of peptide uniformly enriched with 13C and 15N. Biochemistry 37, 4782–4790.

Malencik, D.A., Anderson, S.R., 1983. High affinity binding of the mastoparans by calmodulin. Biochem. Biophys. Res. Commun. 114, 50–56.

Mendes, M.A., de Souza, B.M., Palma, M.S., 2005. Structural and biological characterization of three novel mastoparan peptides from the venom of the neotropical social wasp Protopolybia exigua (Saussure). Toxicon 45, 101–106.

Mizuno, K., Nakahata, N., Ohizumi, Y., 1998. Characterization of mastoparan-induced histamine release from RBL-2H3 cells. Toxicon 36, 447–456.

Morris, A.L., MacArthur, M.W., Hutchinson, E.G., Thornton, J.M., 1992. Stereochemical quality of protein structure coordinates. Proteins 12, 345–364.

Murayama, T., Oda, H., Nomura, Y., 1996. Pertussis toxin-insensitive effects of mastoparan, a wasp venom peptide, in PC12 cells. J. Cell. Physiol. 169, 448–454.

Nakajima, T., Uzu, S., Wakamatsu, K., Saito, K., Miyazawa, T., Yasuhara, T., Tsukamoto, Y., Fujino, M., 1986. Amphiphilic peptides in wasp venom. Biopolymers 25 (Suppl.), S115–S121.

Ohara-Imaizumi, M., Nakamichi, Y., Ozawa, S., Katsuta, H., Ishida, H., Nagamatsu, S., 2001. Mastoparan stimulates GABA release from MIN6 cells: relationship between SNARE proteins and mastoparan action. Biochem. Biophys. Res. Commun. 289, 1025–1030.

Ohki, S.Y., Yazawa, M., Yagi, K., Hikichi, K., 1991. Mastoparan binding induces Ca(2+)-transfer between two globular domains of calmodulin: a 1H NMR study. J. Biochem. (Tokyo) 110, 737–742.

Otwinowski, Z., Minor, W., 1997. Processing of X-ray diffraction data collected in oscillation mode. Methods Enzymol. 276, 307–326.

Park, N.G., Yamato, Y., Lee, S., Sugihara, G., 1995. Interaction of mastoparan-B from venom of a hornet in Taiwan with phospholipid bilayers and its antimicrobial activity. Biopolymers 36, 793–801.

Sandvik, A.K., Dockray, G.J., 1999. Biological activity of carboxy-terminal gastrin analogs. Eur. J. Pharmacol. 364, 199–203.

Sforca, M.L., Oyama Jr., S., Canduri, F., Lorenzi, C.C.B., Pertinhez, T.A., Konno, K., Souza, B.M., Palma, M.S., Neto, J.R., Azevedo Jr., W.F., Spisni, A., 2004. How C-terminal carboxyamidation alters the biological activity of peptides from the venom of the eumenine solitary wasp. Biochemistry 43, 5608–5617.

Shai, Y., 2002. Mode of action of membrane active antimicrobial peptides. Biopolymers 66, 236–248.

Straub, S.G., James, R.F., Dunne, M.J., Sharp, G.W., 1998. Glucose augmentation of mastoparan-stimulated insulin secretion in rat and human pancreatic islets. Diabetes 47, 1053–1057.

Sukumar, M., Ross, E.M., Higashijima, T., 1997. A Gs-selective analog of the receptor-mimetic peptide mastoparan binds to Gs alpha in a kinked helical conformation. Biochemistry 36, 3632–3639.

Vagin, A., Teplyakov, A., 1997. MOLREP: an automated program for molecular replacement. J. Appl. Cryst. 30, 1022–1025.

Wang, F., Liu, X., Li, H., Lang, X., Peng, H., Liu, S., Jiang, T., 2006. Crystallization and preliminary X-ray diffraction analysis of three mastoparans. Protein Pept. Lett. 13, 629–631.

Wu, T.M., Chou, T.C., Ding, Y.A., Li, M.L., 1999. Stimulation of TNF-alpha, IL-1beta and nitrite release from mouse cultured spleen cells and lavaged peritoneal cells by mastoparan M. Immunol. Cell. Biol. 77, 476–482.

Yajima, Y., Uchino, K., Ito, H., Kawashima, S., 1997. Mastoparan-stimulated prolactin secretion in rat pituitary GH3 cells involves activation of Gq/11 proteins. Endocrinology 138, 1949–1958.

Yu, K., Kang, S., Kim, S.D., Ryu, P.D., Kim, Y., 2001. Interactions between mastoparan B and the membrane studied by 1H NMR spectroscopy. J. Biomol. Struct. Dyn. 18, 595–606.